A STRATEGY FOR COST-EFFECTIVE COMPENSATION OF PROCESS INDUCED DEFORMATIONS IN COMPOSITE STRUCTURES

Maximilian Lipcan[1,2], Johannes Mattheus Balvers[1], Mathias Peter Hartmann[2,3]

[1]Airbus Helicopters Deutschland GmbH, Industriestr. 4, 86609 Donauwörth, Germany
[2]Technical University of Munich, Department of Mechanical Engineering, Chair for Carbon Composites, Boltzmannstr. 15, 85748 Garching, Germany
[3]Corresponding author: hartmann@lcc.mw.tum.de; tel. +49 89 289 10313

Keywords: Manufacturing Process Simulation, Process Induced Deformation (PID), Mould Compensation

Abstract
Undesired deviations of the geometry "as built" from the nominal geometry "as designed" are inherent to composite structures made of carbon fibre reinforced plastics. Compensation measures derived from finite element simulations can be implemented in the tooling design. Though, simulated deformation fields may not completely impose a risk of deficient mountability. The industry's goal is therefore to filter only for the relevant modes with respect to the part's assembly process. To this end, a selective compensation of virtual deformation data needs to be derived. The method presented here is implemented as several consecutive filter steps, using Python scripting and ABAQUS. First the simulated displacements are compared against the part's individual tolerance envelope. In a second step, a virtual assembly calculates whether apparent deformations can be accounted for during the part's mounting using allowable rigging loads. Critical deviations exceeding still the tolerance limits are then isolated. In the last step, the derived geometrical compensation for each criticality undergoes a mould feasibility check and cost analysis. A numerical proof of concept for a generic integral structure demonstrates the applicability and effectiveness of the developed strategy.

1. Introduction

Stemming from the trinity of material, design and process, there are several drivers distorting parts made of carbon fibre reinforced plastics (CFRP) during production. This deviation causes additional unwanted efforts: extensive fitting of such parts in the assembly and/or possibly costly tooling rework. Utilizing simple analytical models to predict the occurring deformation, some mould designs can be modified to restore the part's geometrical fidelity [1]. In recent years, several finite element (FE) models with different degrees of scope have been developed to calculate process-induced deformations (PID) for more complex geometries [2, 3, 4, 5]. Utilizing the data from the simulation, the tooling design may be adapted in such a way that the final "as-build" shape of the CFRP parts after manufacturing is within allowable tolerances of the nominal "as-designed" geometry [6]. Thus, addressing manufacturing deviation already during the initial phase of mould design can potentially reduce fitting efforts and hence costs at a later stage.
To efficiently use the calculated displacement fields in tooling design optimization, the simulated

information needs to be reduced first. Only modes and regions relevant for and applicable to redesigning tooling surfaces, should be transferred.
In literature, the effectiveness of compensation measures has been proved at different levels: Zhu et al. optimized the design for flat, cylindrical and l-shaped laminates to counteract occurring process-induced deformations [7]. Kappel showed that using the inverse displacement data of a fairly simple numerical approach as a tooling compensation can even reduce the spring-in from 1.50° to a range of ±0.25° [8]. Wucher et al. validated their compensation methodology by manufacturing both the compensated and initial geometry of a curved C-spar. The study evidenced that for this part with a compensation, retrieved from a path dependent model, 90% of the deformation is accounted for [9]. A similar result was achieved for an integral RTM structure using the even simpler phenomenological approach [6].
Reaching for a complete compensation may lead, however, to overly complex and hence not rational mould design changes. At an industrial level, the goal of such a compensation should, however, be the enable of smooth fitting of the as-built part with minimal design change effort. Apparently, there is no such method currently available for analysing simulated deformation data, based on the partï¿½s individual assembly situation. That is, to take into account the tolerance envelope and allowable assembly forces for isolating only the critical deformations. This would then allow for a selective and hence cost-effective tooling compensation, suitable for an industrial deployment.
In the following, a method to filter numerical deformation data with respect to the part's individual assembly situation and process is presented. First the relevant joining techniques and their tolerance requirements are introduced briefly. Subsequently, the idea of the selective compensation is detailed. For the established context, the criticality is defined together with its required analysis steps (including the implementation strategy within an established dataflow from CAE to CAD). In a proof of concept study the procedure is applied to a generic integral structure.

2. Method

2.1. Description of approach

The analysis steps, as displayed in Fig. 1, identify in three filtering steps the critical deformations case-specific for the assembly of integral helicopter structures. Firstly, the simulated deformation is filtered by comparing it with the present tolerances of the assembly. In subsequent simulation step, each area of the exceeding deformation is pushed back into an acceptable range. With the resulting forces to do so,the deformations is filtered in a second loop. The remaining displacements after the assembly force analysis are separated area-wise and for each a geometrical compensation is derived. Each of these compensations is subjected to the third filter in which its realization in the current mould concept is assessed. To verify the remaining compensation(s), a final loop of deformation and assembly is simulated with the newly obtained mesh (for the corrected geometry). Finally, the data can be transferred with a previously investigated interface to the tooling design [10].
Within the context of analysing shape deviations for production and assembly, criticality defines itself as of the following qualities:

Tolerance analysis: The deviation violate geometrical, shape or positional tolerances of the part.

Mounting analysis: Rigging the deformed part exceeds the allowable loads.

Tooling design feasibility: The derived geometrically compensated shape can be realised cost-efficiently for the existing tooling concept.

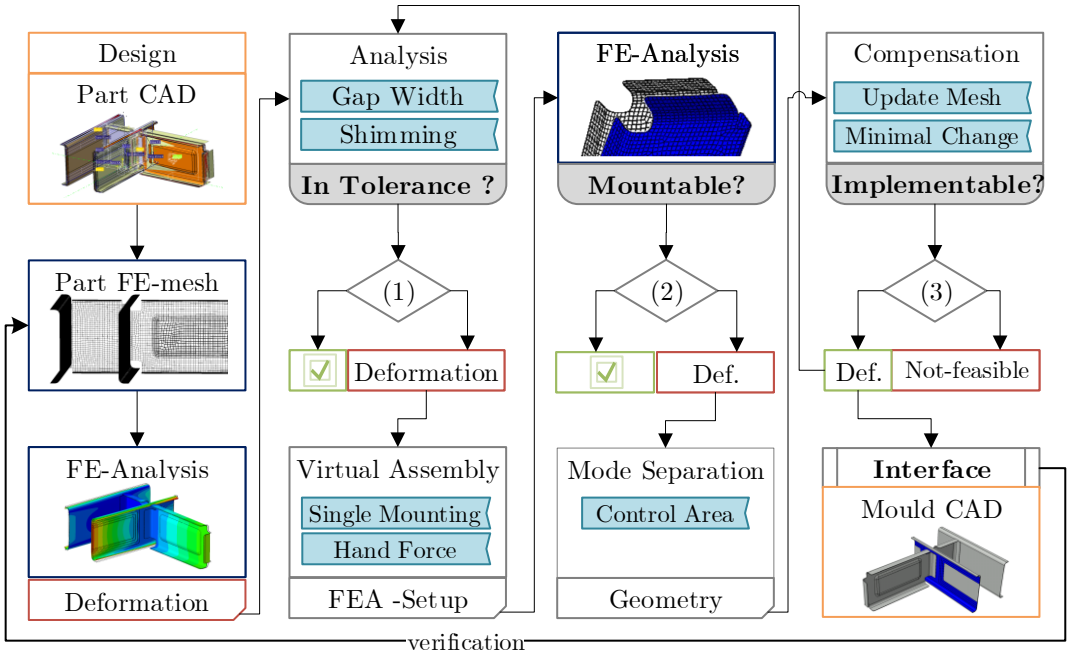

Figure 1. Criticality analysis for the deformation of a integral helicopter structure.

2.2. Tolerances and mounting of structural helicopter parts

The scope here is to identify the criticality of deformations for mounting structural helicopter parts in a small-scale production series (less than 50 parts per year). Due to the inherent variation arising from manual production (autoclave curing of manually laid up prepreg), a so-called "shimming" step is necessary in the assembly. As sketched in Fig. 2, strict tolerances are imposed on the gap width between the contact surfaces of the adjacent parts in the assembled position [11]. An overlap of the two parts results in additional part rework or, in the worst case, in scrapping and part rebuilding. If the gap exceeds a certain limit, a solid shim is needed as well to accompany the liquid one, increasing the processing time by about 30% [12]. Preferably, a gap width within the liquid shimming range is desired to minimize additional assembly effort.
Since the assembly into the rig is performed manually, some deformation can be accounted for by enforcing a mountable position by the worker. The extent is, however, bounded by the defined allowable mounting loads. Its threshold is derived, according to [6], from the maximal permissible manual load. The investigated integral structure relies on a tooling concepts of multiple relatively small moulds and cores. Thus, the costs of a potential geometrical compensation are determined primarily by the number affected moulds, respectively preforms. The shape and extent of a change is considered secondary here.

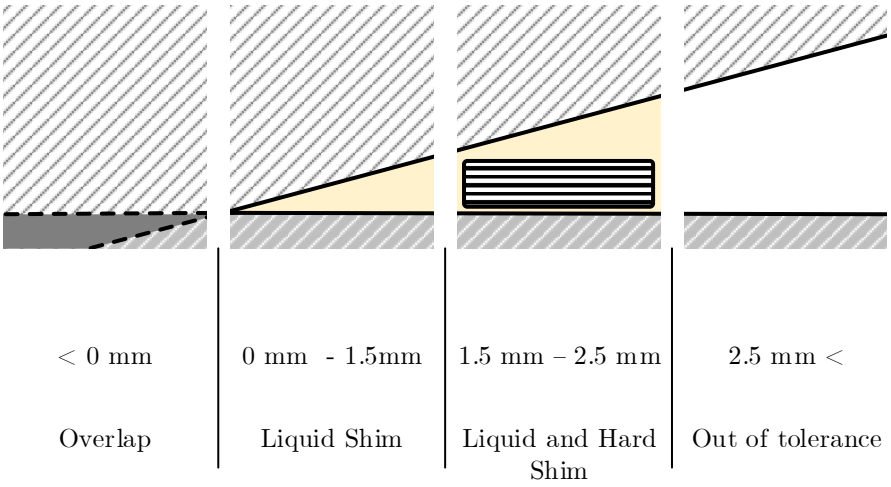

Figure 2. Shimming effort in relation to the gap width between two adjacent parts [11].

2.3. Assumptions and limitations

Based on the presented process and environment (section 2.2), the following assumptions and limitation are made:

1 Tolerance analysis

- The shim gap tolerances are applied only to surfaces which are in contact to other parts, the so-called 'assembly surfaces'.
- The tolerance criterion is the gap width, i.e the displacement fraction normal to the surface.
- No shape and only limited position tolerances are applied.
- There is both an upper and lower tolerance threshold.

2 Virtual mounting analysis

- Manual assembly is the mounting method with regard to load application.
- Maximal admissible manual force is 70N [13].
- The floating support of the component during assembly allows the usage of isostatic boundary conditions.
- The displacement field is filtered by the occuring forces to bring the deformed shape back into acceptable tolerances.

3 Tooling design feasibility

- Deformation modes are isolated via predefined control areas.
- Due to the tooling concept, a compensation should remain within a single preform.
- The compensation measure is derived and applied to the nominal design shape within the scripting environment.

2.4. Selective compensation

As illustrated in Fig. 3, based on the part's assembly process, there is a given tolerance envelope (red dotted line). A finite element simulation predicts the part's deformed shape after processing. Each nodal displacement is individually compared against this envelope. Thus, the displacement's fraction by which the nodes exceed their allowances (orange) are used to derive a selectively compensated tool surface (blue arrows).

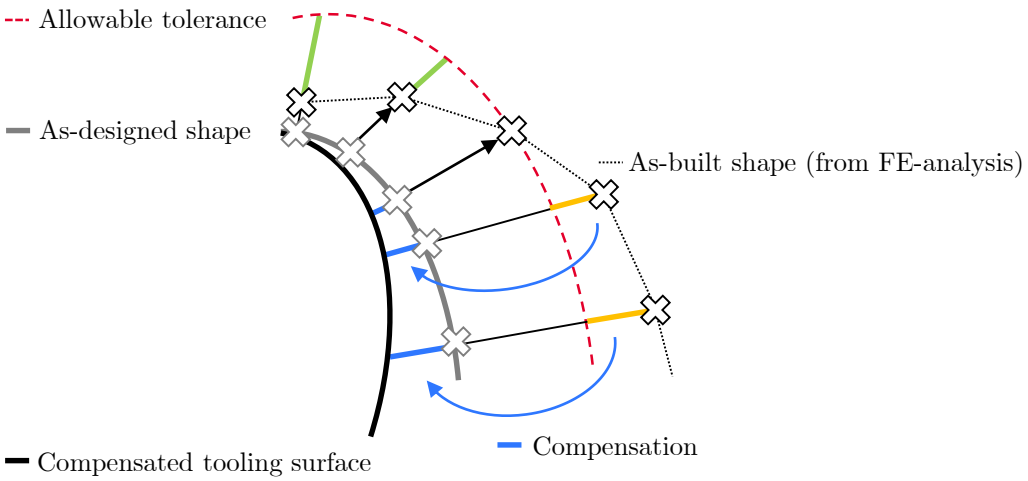

Figure 3. Procedure of a selective displacement compensation.

2.5. Implementation

The single operations within each step, as shown in Fig. 4, are scripted in Python [14, 15]. As the first step, the node coordinates, sets and their elements are retrieved from the input file of an ABAQUS finite element simulation (*.inp). The tolerance values are mapped onto the derived node normal vectors to model the allowable gap width. Subsequently, the displacement vectors are imported from the solver output file (*.odb) and projected onto the normals to determine the simulated gap width. For a new simulation step, a displacement boundary condition is derived in order to move a tolerance violating area into an acceptable range. In this study, the extrema of a tolerance exceeding displacement fraction (both positive and negative) are searched for at each surface. Only one extremum is inverted and applied as a single nodal displacement boundary condition. Subsequently, the induced reaction force can be retrieved without over-constraining the structure. From the result file, the new displacement vectors and reaction forces are imported. The tolerance analysis is repeated to evaluate whether the displaced nodes are now within the envelope without exceeding the allowable forces. Iteratively, more boundary conditions are added to address all occurring tolerance issues. The reaction forces at isostatic boundary condition give estimation on the total introduced load into the part by the adjustments. The procedure is repeated until convergence is reached, i.e. tolerance match cannot be improved further by applying new boundary conditions within given force limits. The remaining exceeding displacement vectors are separated area-wise. For each fraction separately, the geometrical compensation vectors are deduced from the inversion of the final exceeding nodal normal displacement. The mesh is updated with the new locations

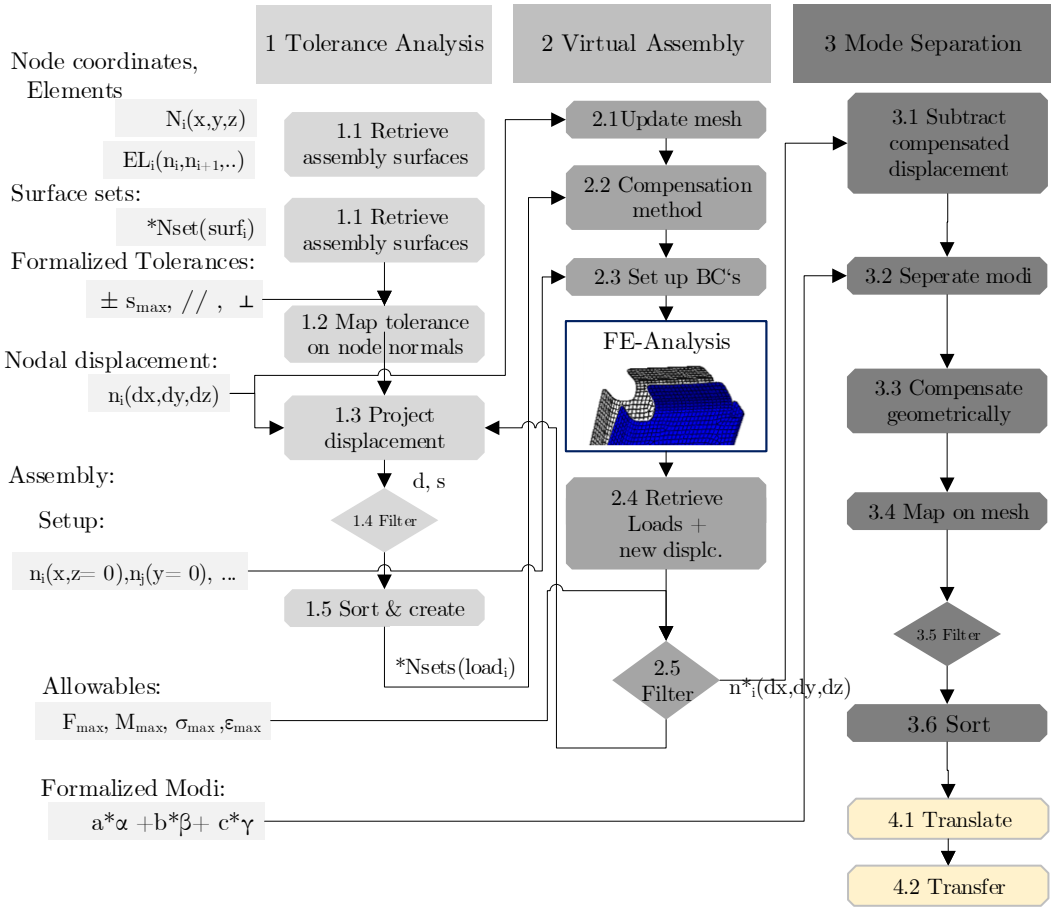

Figure 4. Separation of displacement.

and, if necessary a smoothing merges the new shapes with the initial geometry. The feasibility of each compensation with respect to the producibility of resulting mould design is manually checked. After a rerun of the distortion simulation and a final tolerance assessment, the filtered compensations are translated into the desired file format to be transferred into the mould design.

3. Use case setup

3.1. Assembly analysis

Fig. 5 visualizes the case studies geometry and its eight assembly surfaces 'S1' to 'S8'. The part is an extract of a integral upper deck structure of a helicopter with an artificial high number of design features. Its dimensions are 350mm by 450mm width with a height of 150mm. Two of its five preforms are locally reinforced and one of them features a sandwich core. For the two C-preforms both the horizontal top and bottom areas are defined as assembly surfaces (S5 to S8). Of the connecting preform, no surfaces were selected, since the isostatic boundary conditions are located here. Of the preform with the sandwich core, the top and bottom area were selected as well. The assembly surface S4 area is progressed further into the radial area, whereas surface S3 remains plane.For the outer sandwich flange, two surfaces are selected: the planar flange area

(S1) and its front end (S2) as depicted in the magnification (green box in Fig. 5).
The deformed part is analysed with regard to the gap tolerances as given in Table 1. For the proof of concept here, the values were reduced by about 50 % compared to those given in [11]. The two acceptable fields (green and orange) represent gap widths which can be shimmed.

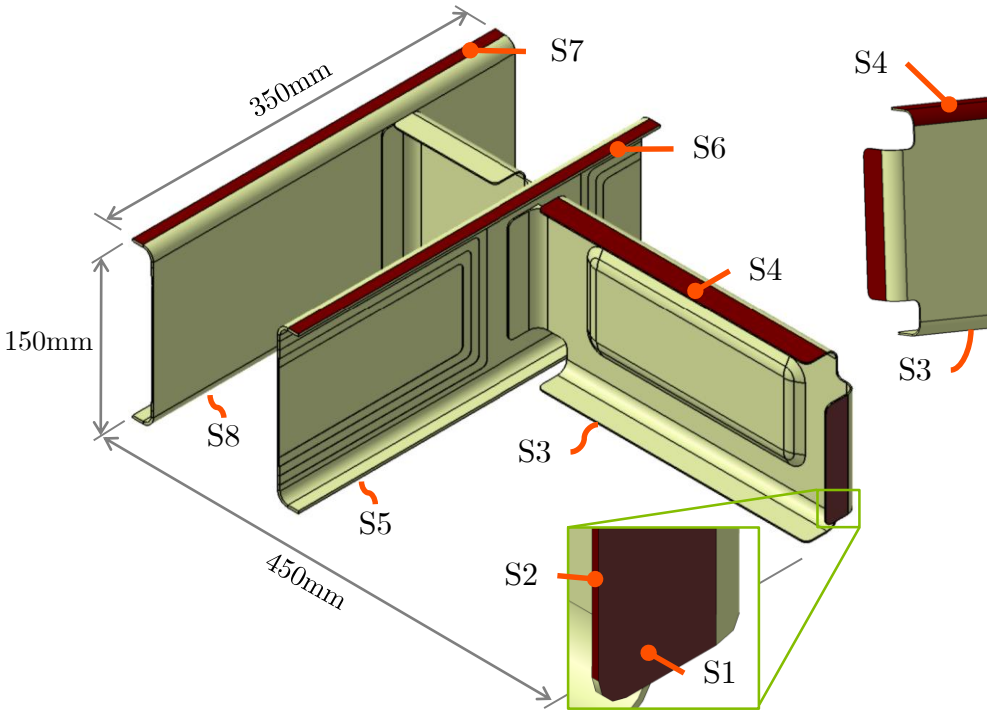

Figure 5. Defined assembly surfaces.

Table 1. Colour code and rework effort of gap width thresholds.

#	Rework	Gap width	Colour
Tol0	Excess	< 0.0 mm	
Tol1	Liquid Shim	0.0 - 0.7 mm	
Tol2	Solid Shim	0.7 - 1.3 mm	
Tol3	Out-of-tolerance	> 1.3 mm	

3.2. Manufacturing distortion simulation

To predict occurring process induced deformations, a phenomenological simulation is performed in ABAQUS as a one-step quasi-static cooldown simulation from process to room temperature on the composite part shown in Fig. 5 (here $\Delta T = 160K$) [2]. The enhanced coefficient of thermal expansion is the sum of the thermal strain and a value of the equivalent strains caused by the chemical cure shrinkage of the epoxy resin [6]. The various composite layups use two types of reinforcements: a unidirectional reinforcement (UD) ply and a woven fabric. In this study, one layer of linear eight node brick elements with incompatible modes (C3D8I) is used per ply, resulting in four to eight elements through the thickness. Additionally, isotropic wedge

elements (C3D6) are used for resin pockets present at ply drop-offs. In order to receive the free deformation of the part, isostatic boundary conditions are applied by restricting the displacement on three nodes of one element. The calculated deformation is shown in Fig. 6. The location of support is marked with a white 'x'.
The part deforms both globally and locally: the two C-frames and the sandwich frame rotate around the z-axis due to spring-in effects at the radial connection between the preforms (purple arrows). Additional the top and bottom ends of all C-frames spring inwards as well (orange arrows). A high number of UD plies are located only at the inner side of the C-frames radii creating an unsymmetrical layup in this area. Thus, a warping occurs along the complete length of the middle C-Frame, especially at the free front end (blue arrow and section cut "B-B" in Fig. 6 (b)).

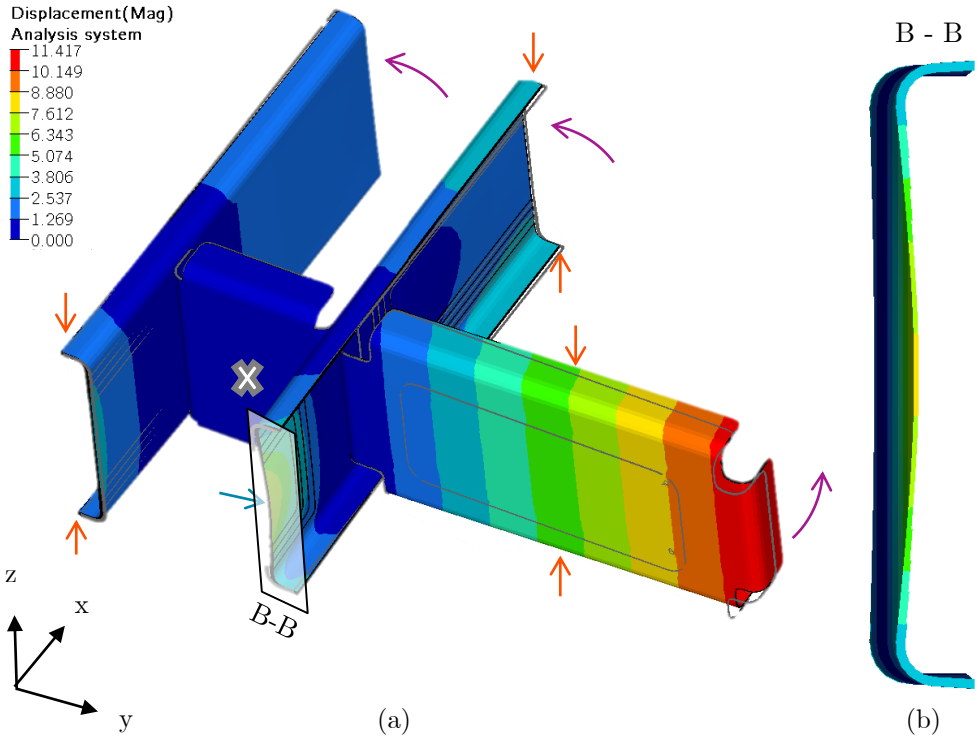

Figure 6. Displacement result of (a) generic integral structure and (b) centre c-preform side view.

4. Results

The results of the initial deformation simulation step are classified into the different tolerance ranges of Table 1. For the defined eight assembly surfaces, the result is summarized in Fig. 7. Each bar represents the range of tolerances for one assembly surface, i.e. the normal displacement distribution ratio per surface. Additionally, for each tolerance field on a surface, the average normal displacement value is shown. For control surface S4 as an example, 60% of the simulated displacement values lie within the desired field of 0.0mm - 0.7mm and the average displacement of this 60% fraction is 0.518 mm. About 8% of the normal displacement values lie within the tolerance field 'tol2' and the remaining 32 % are 'out-of-tolerance'.
The two outer most surfaces of the sandwich preform (S1 and S2) are both violating the tolerances severely due to the spring-in of the complete preform (see Fig. 6). Especially for surface

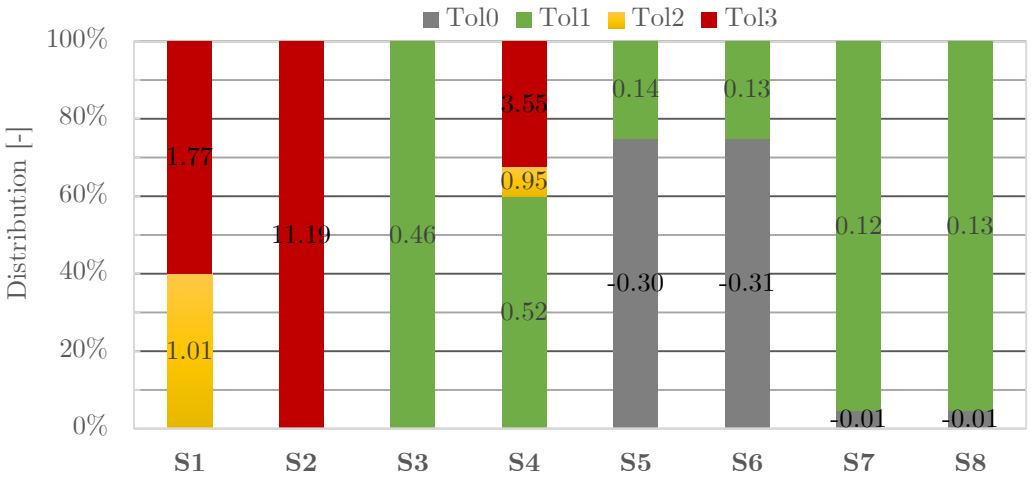

Figure 7. Initial tolerance distribution and average normal displacement per field of each assembly surface after the deformation simulation.

S2, for which the nodal normals point in the main deformation direction, the average displacement is about 11 mm. The normal displacement of surface S1 mainly results from the radial movement of the complete sandwich preform. Surface S4 exhibits a tolerance violation whereas surface S3 does not. In the radial area the node normals share a direction vector with the main deformation direction. Both surfaces S5 and S6 display a great amount of displacement into an overlap. Whereas surfaces S7 and S8 show a low average displacement value and only a small percentage (<5%) exceeding any tolerances.
After five loops of assembly simulations and tolerance assessments, the final tolerance distribution is archived, as presented in Fig. 8. A geometrical compensation was applied to the preform

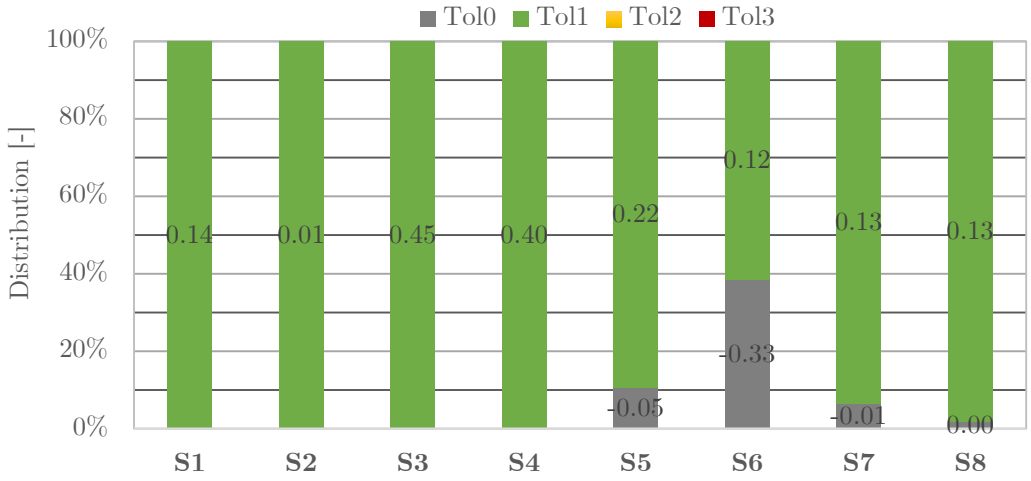

Figure 8. Tolerance distribution and average normal displacement per field of each surface after the deformation and assembly simulation of the compensated geometry.

of surface S5 and S6. Whereas the displacement of the surface S5 lies now within the acceptable range, for surface S6 merely 5% of the displacement values changed into the acceptable range. Fig. 9 shows the location and normal displacement of ssurface S6. It can be seen, that the exceeding nodes are mostly localized at the far edge (x = 250mm) and not uniform over the complete flange. At this location there is also the maximum warping occurring of the complete

preform, as seen in Fig. 6 (b). At an x coordinate of about 25 mm, a fraction of exceeding values occurs now after the compensation.

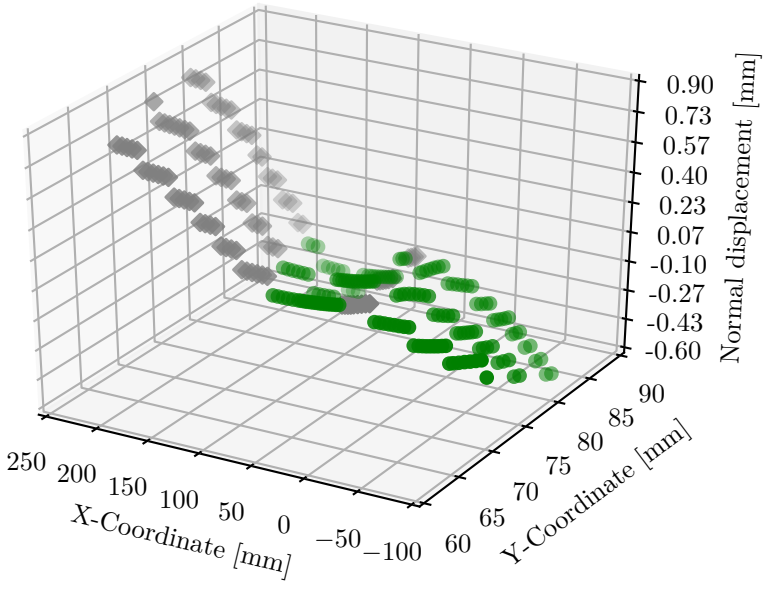

Figure 9. Normal displacement of the compensated assembly surface S6 after the deformation and assembly step.

5. Discussion

In total, the developed method succeeds: Of the eight surfaces that initially violated their gap tolerances, only for two a geometrical compensation was actually needed. The other six surfaces can still be assembled using admissible mounting forces between 1N and 50N. Concerning the geometrical compensation, mixed results were obtained. In accordance with [9], if the deformation mode is dominated by warpage, a mirroring compensation did not succeed completely: for the bottom surface S5, the applied compensation counteracted the occurring deformation and the tolerance fit increased, whereas for the surface on the opposite side of the same preform, the fit did not increase significantly, especially around the warpage deformed area (Fig 6 (b)). Here, a more detailed study into the compensation of such warpage driven deformation modes is recommended.

Acknowledgements

The study was performed in the framework of the LuFo project 'IPRO' funded by the German Federal Ministry for Economic Affairs and Energy (BMWi).

References

[1] Lalit K. Jain, Meng Hou, Lin Ye, and Yiu-Wing Mai. Spring-in study of the aileron rib manufactured from advanced thermoplastic composite. *Composites Part A: Applied Science and Manufacturing*, 29(8):973 – 979, 1998.

[2] Satish K. Bapanapalli and Lloyd V. Smith. A linear finite element model to predict processing-induced distortion in frp laminates. *Composites Part A: Applied Science and Manufacturing*, 36(12):1666 – 1674, 2005.

[3] A. Johnston, R. Vaziri, and A. Poursartip. A plane strain model for process-induced deformation of laminated composite structures. *Journal of Composite Materials*, 35(16):1435–1469, 2001. cited By 155.

[4] J.M. Svanberg and J.A. Holmberg. Prediction of shape distortions part i. fe-implementation of a path dependent constitutive model. *Composites Part A: Applied Science and Manufacturing*, 35(6):711–721, 2004. cited By 101.

[5] Nima Zobeiry, Reza Vaziri, and Anoush Poursartip. Computationally efficient pseudo-viscoelastic models for evaluation of residual stresses in thermoset polymer composites during cure. *Composites Part A: Applied Science and Manufacturing*, 41(2):247 – 256, 2010.

[6] M. P. Hartmann. *Analysis and Compensation of Process Induced Deformations in Composite Structures*. Technicial University of Munich, 2016.

[7] Q. Zhu and P.H. Geubelle. Dimensional accuracy of thermoset composites: Shape optimization. *Journal of Composite Materials*, 36(6):647–672, 2002. cited By 25.

[8] Erik Kappel. Compensating process-induced distortions of composite structures: A short communication. *Composite Structures*, 192:67 – 71, 2018.

[9] B. Wucher, Ph. Martiny, F. Lani, T. Pardoen, C. Bailly, and D. Dumas. Simulation-driven mold compensation strategy for composites: Experimental validation on a doubly-curved part. *Composites Part A: Applied Science and Manufacturing*, 102:96 – 107, 2017.

[10] Maximilian Lipcan. Interface evaluation for efficient integration of manufacturing distortion simulation results in an industrial design process. Linköping, 2016. Swerea Sicomp.

[11] Dieter Meiners. *Beitrag zur Stabilität und Automatisierung von CFK-Produktionsprozessen*. Universitätsbibliothek Clausthal, 2007.

[12] C. Dannenberg. A tool for trade-off assessment on simulation based compensation of process induced deformations of composite structures. Master's thesis, Technical University of Munich, 2015.

[13] U. Steinberg and F. Liebers. Manuelle arbeit ohne schaden: Grundsätze und gefährdungsbeurteilung, 2014.

[14] T. E. Oliphant. Python for scientific computing. *Computing in Science Engineering*, 9(3):10–20, May 2007.

[15] S. Van Der Walt, S.C. Colbert, and G. Varoquaux. The numpy array: A structure for efficient numerical computation. *Computing in Science and Engineering*, 13(2):22–30, 2011. cited By 829.